

# Oscillating scalar potential and its implications for cosmic neutrino background searches

Yechan Kim<sup>1,\*</sup> and Hye-Sung Lee<sup>1,†</sup>

<sup>1</sup>*Department of Physics, Korea Advanced Institute of Science and Technology, Daejeon 34141, Korea*  
(Dated: March 2025)

We propose a novel mechanism in which an external oscillatory wave modulates the mass-squared term of a scalar potential, periodically switching its sign. As a result of this “potential oscillation,” the vacuum transitions between symmetry-broken and symmetry-restored phases. This repeated toggling leads to a time-varying vacuum state with rich phenomenological consequences, driven by the scalar field’s couplings to other sectors. As a concrete illustration, we demonstrate how these oscillations can open a new avenue for probing the cosmic neutrino background.

*Introduction* — Depending on the shape of a scalar potential, spontaneous symmetry breaking may occur, giving masses to particles coupled to the scalar field. This underlies mass generation in the Standard Model (SM) of particle physics [1–3].

Here, we propose a new mechanism in which the scalar potential oscillates due to coupling with external waves, such as wave-like dark matter (wave DM). The shape of the potential itself oscillates at the frequency of the external wave. This “potential oscillation” can periodically shift the vacuum state, causing the symmetry to break during one interval of time and be restored during another.<sup>1</sup>

Such an oscillation in symmetry breaking yields a remarkably simple yet distinctive phenomenology. To illustrate this with a concrete example, we focus on the still-mysterious neutrino mass sector. If the neutrino’s Majorana mass arises through this mechanism, the resulting modulation could allow searches for cosmic neutrinos, analogous to the annual modulation searches employed in dark matter experiments.

*Potential oscillation* — When a scalar field acquires a nonzero vacuum expectation value (VEV) under a spontaneously broken symmetry, it can provide mass to particles. For definiteness, consider the following potential for a real scalar  $\phi$ :

$$V(\phi) = \frac{1}{2} \mu^2(t) \phi^2 + \frac{1}{4} \lambda \phi^4, \quad (1)$$

where  $\mu^2(t)$  oscillates due to an external wave.

When  $\mu^2(t) > 0$ , the VEV is  $v_\phi = 0$ , and the vacuum retains its  $\mathbb{Z}_2$  symmetry. In contrast, if  $\mu^2(t) < 0$  (tachyonic), the VEV is

$$v_\phi = \pm \sqrt{\frac{-\mu^2(t)}{\lambda}}. \quad (2)$$

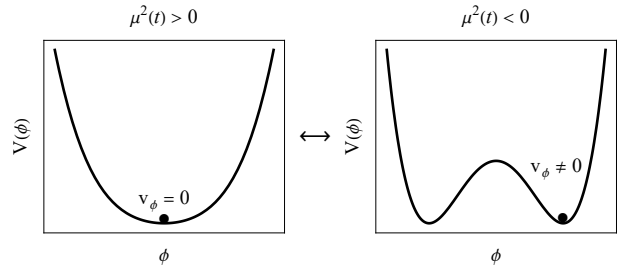


FIG. 1. Schematic representation of the potential oscillation. The sign of  $\mu^2(t)$  changes periodically, inducing transitions between zero and nonzero VEV of  $\phi$ .

If the sign of  $\mu^2(t)$  oscillates over time, the scalar’s VEV periodically switches between zero and nonzero values, as shown schematically in Fig. 1. When  $v_\phi \neq 0$ , the symmetry of the potential is spontaneously broken, and the particles coupled to  $\phi$  become massive. In contrast, when  $v_\phi = 0$ , the symmetry is restored, and these particles become massless.

Such a time-dependent potential can be realized if  $\mu^2$  is generated by an oscillating field, for instance, wave DM [10]. Many recent works have investigated how particle masses can vary if the coupling of the particle with wave DM directly forms a mass [11–44]. In such scenarios, the mass of a particle changes over time, and it vanishes only momentarily when the wave DM field value equals zero.

In contrast, in our mechanism, it is the *coefficient*  $\mu^2$  in  $V(\phi)$  that is induced by wave DM, causing the *shape* of the scalar potential to oscillate. As a result, any particle mass that depends on the scalar’s VEV repeatedly transitions between massive and massless states. Unlike the aforementioned wave DM coupling scenario, here the scalar’s VEV remains zero (restoring the symmetry) for finite intervals whenever  $\mu^2(t)$  is positive.

*Neutrino type oscillation* — As a concrete application, we examine the neutrino sector. If the neutrino’s Majorana mass arises through this mechanism, then, depending on the potential shape at a given time, neutrinos can alternate between a pure Dirac state (where the Ma-

<sup>1</sup> A time-dependent potential has been investigated in the context of reheating after inflation [4–6] and in axion production [7]. Also, symmetry restoration in the early universe via finite temperature effects has been studied [8, 9]. However, periodic symmetry restoration has not been discussed previously.

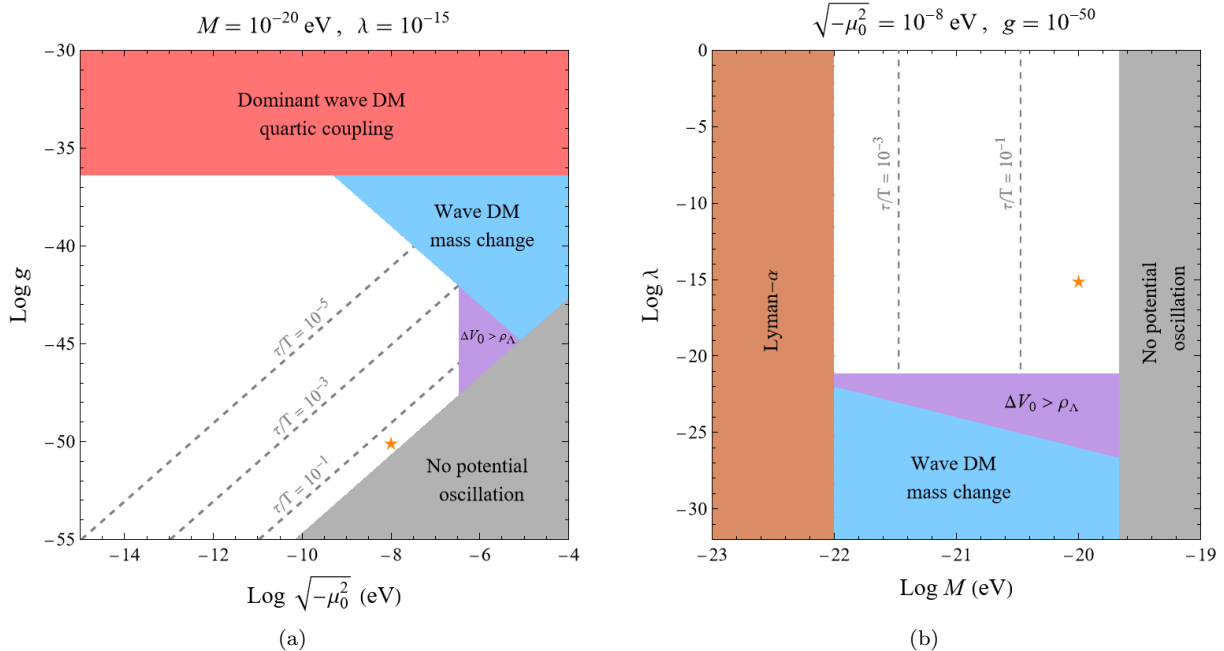


FIG. 2. (a) Parameter space in the  $(\sqrt{-\mu_0^2}, g)$  plane, where  $\mu_0$  is the tachyonic bare mass of the singlet  $\phi$  and  $g$  is the mixing strength of  $\phi$  and  $\Phi$ . (b) Parameter space in the  $(M, \lambda)$  plane, where  $M$  is the mass of the wave DM  $\Phi$  and  $\lambda$  is the singlet  $\phi$ 's quartic coupling. Lines corresponding to the Majorana time ratio  $\tau/T = \{10^{-1}, 10^{-3}, 10^{-5}\}$  are shown, where  $T = 2\pi/M$ . The star denotes the benchmark point used in Fig. 3. In (b), the constraint from the dominant quartic coupling of the wave DM is weaker than the Lyman- $\alpha$  bound.

Majorana mass is zero) and a Majorana state (where the Majorana mass is nonzero).

Although time-dependent neutrino masses induced by wave-like dark matter are not new [12, 14–30, 32–44], our approach differs in that it is not the mass term itself that oscillates, but rather the potential—whose spontaneous symmetry breaking generates the mass—that oscillates. As a result, neutrinos can spend part of the time in a Majorana state and a comparable fraction in a pure Dirac state. This leads to distinctive predictions, including possible periodic modulation signals in the cosmic neutrino background (C $\nu$ B), which we discuss below.

Consider the scalar Lagrangian and its interactions with other fields, which include a real singlet scalar  $\phi$ , a real wave DM scalar  $\Phi$ , and a Majorana neutrino  $N$ :

$$\mathcal{L}_{\text{scalar}} = -\frac{1}{2}(\mu_0^2 + g\Phi^2)\phi^2 - \frac{\lambda}{4}\phi^4 - \frac{1}{2}M^2\Phi^2, \quad (3)$$

$$\mathcal{L}_{\text{int}} = -\frac{y}{2}\phi\bar{N}^c N + \text{h.c.} \quad (4)$$

We assume bare term  $\mu_0^2 < 0$  (tachyonic) and introduce the scalar mixing coupling  $g$  between the singlet scalar  $\phi$  and the wave DM  $\Phi$ . Note that  $\mu^2(t)$  in Eq. (1) is effectively replaced by

$$\mu_{\text{eff}}^2 \equiv \mu_0^2 + g\Phi^2, \quad (5)$$

which oscillates over time. Both  $g$  and  $\lambda$  are positive, and  $M$  is the wave DM mass. The terms in Eq. (4) generate the Majorana mass  $M_N = y v_\phi$ .

For simplicity, we consider a Lagrangian with a discrete  $\mathbb{Z}_2$  symmetry. However, the same principle applies to continuous symmetries, such as a global  $U(1)_L$  associated with lepton number.

The equation of motion for wave DM  $\Phi$  in an expanding universe, assuming spatial homogeneity, is

$$\ddot{\Phi} + 3H\dot{\Phi} + M_\Phi^2\Phi = 0, \quad (6)$$

where  $H$  is the Hubble parameter, and  $M_\Phi = \sqrt{M^2 + g\phi^2}$  is the effective mass of the wave DM. In the current epoch, Hubble friction is negligible, so  $\Phi(t)$  oscillates as

$$\Phi(t) = \frac{\sqrt{2\rho_\Phi}}{M_\Phi} \cos(M_\Phi t), \quad (7)$$

where  $\rho_\Phi$  is the wave DM density. We assume the wave DM  $\Phi$  constitutes the nearly entire local dark matter density,  $\rho_{\text{dm}}^0 = 0.3 \text{ GeV/cm}^3$ , at present. The wave DM mass ranges from approximately  $10^{-22} \text{ eV}$  (brown bound in Fig. 2 as constrained by Lyman- $\alpha$  forest data) up to about  $30 \text{ eV}$  (which ensures harmonic oscillation behavior) [10]. Meanwhile, the singlet  $\phi$ 's energy density is much smaller, because its large mass suppresses its production in the early universe. Further details on these

points, including the full equations of motion (which include the singlet scalar  $\phi$ ) and the fast-roll condition, are provided in the Supplemental Material.

The sign of the singlet  $\phi$  potential's quadratic term,  $\mu_{\text{eff}}^2$ , flips if  $-\mu_0^2 < g\Phi^2$ , making  $\mu_{\text{eff}}^2 > 0$ . In that case, the symmetry remains unbroken ( $v_\phi = 0$ ) and the neutrino is a pure Dirac particle. Conversely, if  $-\mu_0^2 > g\Phi^2$  ( $\mu_{\text{eff}}^2 < 0$ ), the symmetry is broken and the singlet acquires a nonzero VEV:

$$v_\phi = \pm \sqrt{\frac{-(\mu_0^2 + g\Phi^2)}{\lambda}}, \quad (8)$$

generating a nonzero Majorana mass.

*Conditions and constraints* — Figure 2 shows various constraints on  $(\sqrt{-\mu_0^2}, g)$  and  $(M, \lambda)$ .

For the potential to oscillate, the wave DM amplitude must exceed the magnitude of the singlet  $\phi$ 's tachyonic bare mass (gray bound in Fig. 2), thereby allowing  $\mu_{\text{eff}}^2 > 0$ :

$$-\mu_0^2 < g\Phi_{\text{max}}^2 = \frac{2g\rho_\Phi}{M_\Phi^2}. \quad (9)$$

When this holds, there is a time interval  $\tau$  in each period  $T = 2\pi/M_\Phi$  of the wave DM  $\Phi$  during which the neutrino is Majorana (rather than pure Dirac), given by

$$\sin^2\left(\frac{\pi}{2} \frac{\tau}{T}\right) = \frac{-\mu_0^2}{g\Phi_{\text{max}}^2}. \quad (10)$$

We refer to  $\tau/T$  as the Majorana time ratio. If Eq. (9) is not satisfied, the potential oscillation does not occur and the neutrino is Majorana at all times ( $\tau/T = 1$ ).

A nonzero VEV of the singlet  $\phi$  can shift  $M_\Phi$ , which in turn affects  $\mu_{\text{eff}}^2$ . We keep  $M_\Phi$  nearly constant by requiring  $M^2 > g\phi_{\text{max}}^2$  (blue bound in Fig. 2).<sup>2</sup> Concretely, this condition becomes

$$M^2 > \frac{-g\mu_0^2}{\lambda}. \quad (11)$$

Combining with Eq. (9), one obtains

$$-\mu_0^2 < (2\rho_\Phi \lambda)^{1/2} \quad \text{and} \quad M_N < y \left(\frac{2\rho_\Phi}{\lambda}\right)^{1/4}. \quad (12)$$

For nearly constant  $M_\Phi$  and small  $\tau/T$ , Eq. (10) reduces to  $\tau \simeq \sqrt{-8\mu_0^2/(\rho_\Phi g)}$ , independent of  $M$ .

Possible constraints from loop-level induced quartic couplings of the singlet scalar  $\phi$  and the wave DM  $\Phi$  [45, 46], bounds on the Majorana mass coupling [47],

<sup>2</sup> In general, one could also consider an oscillating effective mass with sizable changes [4–7], but here we focus on the case where  $M_\Phi$  remains nearly constant.

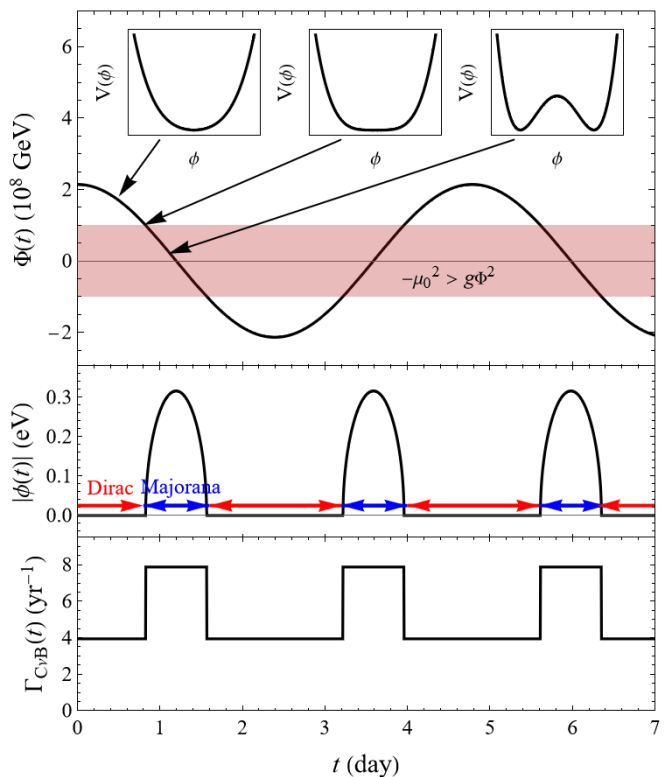


FIG. 3. Time evolution of the wave DM field  $\Phi(t)$ , the singlet scalar potential  $V(\phi)$ , and hence the singlet field  $\phi(t)$ . Benchmark parameters:  $M = 10^{-20}$  eV ( $T = 2\pi/M \simeq 4.8$  days),  $\lambda = 10^{-15}$ ,  $\sqrt{-\mu_0^2} = 10^{-8}$  eV, and  $g = 10^{-50}$ . The potential is tachyonic ( $\mu_{\text{eff}}^2 < 0$ ) inside the red bands, causing the neutrino to become Majorana. Outside those bands, the neutrino is pure Dirac. The frequency changes slightly within the red bands due to the effective wave DM mass, slightly shortening the period. In the bottom panel, the cosmic neutrino background (CνB) detection rate is shown for a 100 g tritium target [48], a Dirac mass  $m_D = 0.1$  eV, and a single neutrino flavor. When the neutrino is Majorana, the detection rate doubles.

and considerations related to the vacuum energy scale are discussed in the Supplemental Material.

In Fig. 3, we illustrate the wave DM and singlet  $\phi$  field evolution for a benchmark point that satisfies all conditions and remains safe from the relevant constraints. It yields a period of several days ( $T \simeq 4.8$  days) and a comparable time ratio of Majorana and Dirac phases ( $\tau/T \simeq 0.3$ ). The singlet scalar  $\phi$ 's nonzero VEV slightly increases  $M_\Phi$  (via  $g\phi^2$ ), slightly speeding up oscillations and shortening the period when  $\mu_{\text{eff}}^2 < 0$ .

#### *Implications for Dirac and Majorana type distinctions*

— Neutrinos' nature (whether Dirac or Majorana) can be probed through two primary approaches [49]. A quasi-Dirac neutrino, characterized by a small ratio of Majorana to Dirac mass ( $M_N \ll m_D$ ), can exhibit properties closely resembling a pure Dirac neutrino ( $M_N = 0$ ) in

some scenarios but not in others. This distinction forms the basis for the two approaches:

(i) Quasi-Dirac (including pure Dirac) vs. Majorana: The first approach involves searching for lepton-number-violating (LNV) processes, such as neutrinoless double beta decay ( $0\nu\beta\beta$ ) [50] or collider signatures of Majorana neutrinos [51, 52]. These processes test whether the Majorana mass is significantly smaller than the Dirac mass (quasi-Dirac as well as pure Dirac). Since an LNV term is expected to be strongly suppressed for quasi-Dirac neutrinos [53, 54], this approach does not strictly require a pure Dirac neutrino, as quasi-Dirac neutrinos can exhibit similar properties.

(ii) Pure Dirac vs. Majorana: The second approach determines whether neutrinos and antineutrinos are identical. A key example is the detection of the cosmic neutrino background ( $C\nu B$ ), which directly probes whether neutrinos are strictly pure Dirac or Majorana. Unlike the first approach, quasi-Dirac neutrinos do not mimic the behavior of pure Dirac neutrinos in this scenario. Naturally, the potential oscillation can play an important role.

The  $C\nu B$  consists of relic neutrinos that decoupled in the early universe, now cooled to  $T_\nu \simeq 0.168$  meV and in a non-relativistic state. Experiments such as PTOLEMY [48, 55, 56] aim to detect the  $C\nu B$  through neutrino capture on tritium ( $\nu + {}^3\text{H} \rightarrow {}^3\text{He} + e^-$ ). In the pure Dirac case, only left-handed helicities contribute, whereas for Majorana neutrinos, both helicity states participate since neutrinos and antineutrinos are indistinguishable. Consequently, the capture rate for Majorana neutrinos is twice that of Dirac neutrinos,  $\Gamma_{C\nu B}^M = 2\Gamma_{C\nu B}^D$ .

Figure 3 illustrates the modulation of the detection rate under neutrino oscillations between Dirac and Majorana states, following the formalism of Ref. [57]. The parameters used include a 100 g tritium target [48], a Dirac mass of  $m_D = 0.1$  eV, and a single neutrino flavor. Despite the  $\sim 12.3$  yr half-life of tritium beta decay, this does not affect short-timescale modulation analyses. Additionally, the beta-decay background can be subtracted due to its spectral distinction from the  $C\nu B$  capture signal.

Other processes, such as neutrino-antineutrino pair emission ( $X \rightarrow Y + \nu\bar{\nu}$ ) [58–62], also fall under the pure Dirac vs. Majorana category and could, in principle, exhibit modulation if neutrinos oscillate between Dirac and Majorana states, although the effect is suppressed by the small neutrino masses. Further implications for neutrino flavor oscillations, including three active neutrino generations [63], and cosmological considerations such as domain walls [64–69], are discussed in the Supplemental Material.

*Summary and outlook* — We have introduced a potential oscillation mechanism that periodically breaks and restores symmetry via an externally modulated

scalar potential. Our primary focus in its application is neutrino physics, but it extends naturally to other new physics frameworks such as a dark photon scenario with gauge symmetry. This mechanism provides an elegant route to realize time-dependent mass structures and offers rich phenomenological signatures, such as modulated cosmic neutrino background detection rates.

We thank J. Lee and J. Yi for their helpful comments. This work was supported in part by the National Research Foundation of Korea (Grant No. RS-2024-00352537).

---

\* cj7801@kaist.ac.kr

† hyesung.lee@kaist.ac.kr

- [1] F. Englert and R. Brout, *Phys. Rev. Lett.* **13**, 321 (1964).
- [2] P. W. Higgs, *Phys. Rev. Lett.* **13**, 508 (1964).
- [3] G. S. Guralnik, C. R. Hagen, and T. W. B. Kibble, *Phys. Rev. Lett.* **13**, 585 (1964).
- [4] L. Kofman, A. D. Linde, and A. A. Starobinsky, *Phys. Rev. Lett.* **73**, 3195 (1994), arXiv:hep-th/9405187.
- [5] L. Kofman, A. D. Linde, and A. A. Starobinsky, *Phys. Rev. D* **56**, 3258 (1997), arXiv:hep-ph/9704452.
- [6] B. A. Bassett and S. Liberati, *Phys. Rev. D* **58**, 021302 (1998), [Erratum: *Phys. Rev. D* **60**, 049902 (1999)], arXiv:hep-ph/9709417.
- [7] R. T. Co, L. J. Hall, and K. Harigaya, *Phys. Rev. Lett.* **120**, 211602 (2018), arXiv:1711.10486 [hep-ph].
- [8] D. A. Kirzhnits and A. D. Linde, *Phys. Lett. B* **42**, 471 (1972).
- [9] E. Senaha, *Symmetry* **12**, 733 (2020).
- [10] L. Hui, *Ann. Rev. Astron. Astrophys.* **59**, 247 (2021), arXiv:2101.11735 [astro-ph.CO].
- [11] K. Van Tilburg, N. Leefer, L. Bougas, and D. Budker, *Phys. Rev. Lett.* **115**, 011802 (2015), arXiv:1503.06886 [physics.atom-ph].
- [12] M. M. Reynoso and O. A. Sampayo, *Astropart. Phys.* **82**, 10 (2016), arXiv:1605.09671 [hep-ph].
- [13] A. Arvanitaki, P. W. Graham, J. M. Hogan, S. Rajendran, and K. Van Tilburg, *Phys. Rev. D* **97**, 075020 (2018), arXiv:1606.04541 [hep-ph].
- [14] A. Berlin, *Phys. Rev. Lett.* **117**, 231801 (2016), arXiv:1608.01307 [hep-ph].
- [15] Y. Zhao, *Phys. Rev. D* **95**, 115002 (2017), arXiv:1701.02735 [hep-ph].
- [16] G. Krnjaic, P. A. N. Machado, and L. Necib, *Phys. Rev. D* **97**, 075017 (2018), arXiv:1705.06740 [hep-ph].
- [17] V. Brdar, J. Kopp, J. Liu, P. Prass, and X.-P. Wang, *Phys. Rev. D* **97**, 043001 (2018), arXiv:1705.09455 [hep-ph].
- [18] H. Davoudiasl, G. Mohlabeng, and M. Sullivan, *Phys. Rev. D* **98**, 021301 (2018), arXiv:1803.00012 [hep-ph].
- [19] J. Liao, D. Marfatia, and K. Whisnant, *JHEP* **04**, 136 (2018), arXiv:1803.01773 [hep-ph].
- [20] F. Capozzi, I. M. Shoemaker, and L. Vecchi, *JCAP* **07**, 004 (2018), arXiv:1804.05117 [hep-ph].
- [21] G.-Y. Huang and N. Nath, *Eur. Phys. J. C* **78**, 922 (2018), arXiv:1809.01111 [hep-ph].

- [22] Y. Farzan, *Phys. Lett. B* **797**, 134911 (2019), arXiv:1907.04271 [hep-ph].
- [23] J. M. Cline, *Phys. Lett. B* **802**, 135182 (2020), arXiv:1908.02278 [hep-ph].
- [24] A. Dev, P. A. N. Machado, and P. Martínez-Miravé, *JHEP* **01**, 094 (2021), arXiv:2007.03590 [hep-ph].
- [25] M. Losada, Y. Nir, G. Perez, and Y. Shpilman, *JHEP* **04**, 030 (2022), arXiv:2107.10865 [hep-ph].
- [26] G.-y. Huang and N. Nath, *JCAP* **05**, 034 (2022), arXiv:2111.08732 [hep-ph].
- [27] E. J. Chun, (2021), arXiv:2112.05057 [hep-ph].
- [28] A. Dev, G. Krnjaic, P. Machado, and H. Ramani, *Phys. Rev. D* **107**, 035006 (2023), arXiv:2205.06821 [hep-ph].
- [29] G.-y. Huang, M. Lindner, P. Martínez-Miravé, and M. Sen, *Phys. Rev. D* **106**, 033004 (2022), arXiv:2205.08431 [hep-ph].
- [30] M. Losada, Y. Nir, G. Perez, I. Savoray, and Y. Shpilman, *JHEP* **03**, 032 (2023), arXiv:2205.09769 [hep-ph].
- [31] J. Guo, Y. He, J. Liu, X.-P. Wang, and K.-P. Xie, *Commun. Phys.* **6**, 225 (2023), arXiv:2206.14221 [hep-ph].
- [32] D. Brzemiński, S. Das, A. Hook, and C. Ristow, *JHEP* **08**, 181 (2023), arXiv:2212.05073 [hep-ph].
- [33] G. Alonso-Álvarez, K. Bleau, and J. M. Cline, *Phys. Rev. D* **107**, 055045 (2023), arXiv:2301.04152 [hep-ph].
- [34] M. Losada, Y. Nir, G. Perez, I. Savoray, and Y. Shpilman, *Phys. Rev. D* **108**, 055004 (2023), arXiv:2302.00005 [hep-ph].
- [35] H. Davoudiasl and P. B. Denton, *Phys. Rev. D* **108**, 035013 (2023), arXiv:2301.09651 [hep-ph].
- [36] T. Gherghetta and A. Shkerin, *Phys. Rev. D* **108**, 095009 (2023), arXiv:2305.06441 [hep-ph].
- [37] Y. ChoeJo, Y. Kim, and H.-S. Lee, *Phys. Rev. D* **108**, 095028 (2023), arXiv:2305.16900 [hep-ph].
- [38] Y. Chen, X. Xue, and V. Cardoso, (2023), arXiv:2308.00741 [hep-ph].
- [39] Y. ChoeJo, K. Enomoto, Y. Kim, and H.-S. Lee, *JHEP* **03**, 003 (2024), arXiv:2311.16672 [hep-ph].
- [40] P. Martínez-Miravé, Y. F. Perez-Gonzalez, and M. Sen, *Phys. Rev. D* **110**, 055005 (2024), arXiv:2406.01682 [hep-ph].
- [41] Y. ChoeJo, K. Enomoto, Y. Kim, and H.-S. Lee, (2024), arXiv:2406.19694 [hep-ph].
- [42] R. Plestid and S. Tevosyan, (2024), arXiv:2409.17396 [hep-ph].
- [43] J.-W. Lee, (2024), arXiv:2410.02842 [hep-ph].
- [44] G. Lambiase, T. K. Poddar, and L. Visinelli, (2025), arXiv:2503.02940 [hep-ph].
- [45] S. R. Coleman and E. J. Weinberg, *Phys. Rev. D* **7**, 1888 (1973).
- [46] M. S. Turner, *Phys. Rev. D* **28**, 1243 (1983).
- [47] A. Gando *et al.* (KamLAND-Zen), *Phys. Rev. C* **86**, 021601 (2012), arXiv:1205.6372 [hep-ex].
- [48] S. Betts *et al.*, in *Snowmass 2013: Snowmass on the Mississippi* (2013) arXiv:1307.4738 [astro-ph.IM].
- [49] C. S. Kim, J. Rosiek, and D. Sahoo, *Eur. Phys. J. C* **83**, 221 (2023), arXiv:2209.10110 [hep-ph].
- [50] W. H. Furry, *Phys. Rev.* **56**, 1184 (1939).
- [51] W.-Y. Keung and G. Senjanovic, *Phys. Rev. Lett.* **50**, 1427 (1983).
- [52] G. Anamiati, M. Hirsch, and E. Nardi, *JHEP* **10**, 010 (2016), arXiv:1607.05641 [hep-ph].
- [53] J. W. F. Valle and M. Singer, *Phys. Rev. D* **28**, 540 (1983).
- [54] M. Doi, T. Kotani, and E. Takasugi, *Prog. Theor. Phys. Suppl.* **83**, 1 (1985).
- [55] E. Baracchini *et al.* (PTOLEMY), (2018), arXiv:1808.01892 [physics.ins-det].
- [56] M. G. Betti *et al.* (PTOLEMY), *JCAP* **07**, 047 (2019), arXiv:1902.05508 [astro-ph.CO].
- [57] A. J. Long, C. Lunardini, and E. Sabancilar, *JCAP* **08**, 038 (2014), arXiv:1405.7654 [hep-ph].
- [58] B. Kayser and R. E. Shrock, *Phys. Lett. B* **112**, 137 (1982).
- [59] R. E. Shrock, *eConf* **C8206282**, 261 (1982).
- [60] J. F. Nieves and P. B. Pal, *Phys. Rev. D* **32**, 1849 (1985).
- [61] A. Fukumi *et al.*, *PTEP* **2012**, 04D002 (2012), arXiv:1211.4904 [hep-ph].
- [62] C. S. Kim, M. V. N. Murthy, and D. Sahoo, *Phys. Rev. D* **105**, 113006 (2022), arXiv:2106.11785 [hep-ph].
- [63] J. A. Casas and A. Ibarra, *Nucl. Phys. B* **618**, 171 (2001), arXiv:hep-ph/0103065.
- [64] Y. B. Zeldovich, I. Y. Kobzarev, and L. B. Okun, *Zh. Eksp. Teor. Fiz.* **67**, 3 (1974).
- [65] P. Sikivie, *Phys. Rev. Lett.* **48**, 1156 (1982).
- [66] A. Vilenkin, *Phys. Rept.* **121**, 263 (1985).
- [67] A. Lazanu, C. J. A. P. Martins, and E. P. S. Shellard, *Phys. Lett. B* **747**, 426 (2015), arXiv:1505.03673 [astro-ph.CO].
- [68] J. C. Fabris and S. V. de Borba Goncalves, *Braz. J. Phys.* **33**, 834 (2003), arXiv:gr-qc/0010046.
- [69] A. Friedland, H. Murayama, and M. Perelstein, *Phys. Rev. D* **67**, 043519 (2003), arXiv:astro-ph/0205520.

## SUPPLEMENTAL MATERIAL

*Dynamics of the singlet scalar* — The coupled equations of motion for the wave DM  $\Phi$  and the singlet scalar  $\phi$  are given by

$$\ddot{\Phi} + 3H\dot{\Phi} + (M^2 + g\phi^2)\Phi = 0, \quad (13)$$

$$\ddot{\phi} + 3H\dot{\phi} + (\mu_0^2 + g\Phi^2)\phi + \lambda\phi^3 = \frac{y}{2}\overline{N^c}N + \text{h.c.} \quad (14)$$

In the current universe, the Hubble friction term is negligibly small, so the wave DM  $\Phi$  oscillates according to Eq. (7) in the main text. The term involving heavy neutrinos on the right-hand side of Eq. (14) can be neglected because their density in the universe is negligible today.

With the singlet  $\phi$  field to track the minimum of its potential, it must roll quickly (i.e., not be in a slow-roll regime). For the singlet scalar potential  $V(\phi)$  from Eq. (3), this fast-roll condition can be written as

$$H\dot{\phi} \sim H \frac{\delta\phi}{H^{-1}} \ll \frac{\partial V(\phi)}{\partial\phi}, \quad (15)$$

where  $\delta\phi$ , the change in  $\phi$  during one Hubble time, is large compared to the field value itself ( $\phi \ll \delta\phi$ ). Under this condition, the inequality simplifies to

$$H^2 \ll (\mu_0^2 + g\Phi^2) + \lambda\phi^2. \quad (16)$$

Since the current Hubble parameter value is  $H_0 \simeq 10^{-33}$  eV, this condition is easily satisfied in the present epoch with appropriate parameter choices. As an example, using the benchmark parameters in Fig. 3 of the main text, the right-hand side of condition (16) evaluates to  $10^{-16}$  eV<sup>2</sup>, fulfilling the fast-roll requirement.

In the unbroken phase, the mass of the singlet scalar  $\phi$  is  $\mu_{\text{eff}}$ , while in the broken phase it is  $\sqrt{-2\mu_{\text{eff}}^2}$ . The change in its mass remains small if  $g$  is sufficiently small.

*Constraints from loop corrections* — Although the Lagrangian in Eq. (3) does not include a quartic term for the wave DM  $\Phi$ , such a term can be generated at the one-loop level via scalar mixing ( $-\frac{1}{2}g\Phi^2\phi^2$ ). If this quartic term dominates, the wave DM energy density would behave like radiation [28, 46]. To maintain predominantly harmonic oscillations of the wave DM  $\Phi$  in the present epoch, the loop-generated quartic term from the Coleman-Weinberg potential [45] must remain smaller than the quadratic term (red bound in Fig. 2 of the main text):

$$\frac{g^2}{16\pi^2}\Phi_{\text{max},0}^4 < \frac{1}{2}M^2\Phi_{\text{max},0}^2, \quad (17)$$

where  $\Phi_{\text{max},0}$  is the present-day wave DM amplitude. This inequality implies

$$\frac{\rho_{\text{dm}}^0 g^2}{4\pi^2} < M^4. \quad (18)$$

Similarly, one-loop corrections to the singlet  $\phi$ 's quartic coupling  $\lambda$  may arise, but they should not significantly alter the bare value of  $\lambda$ . Concretely,

$$\frac{y^4}{16\pi^2} < \frac{\lambda}{4} \quad \text{and} \quad \frac{g^2}{16\pi^2} < \frac{\lambda}{4}. \quad (19)$$

From the first inequality, the upper bound on the Majorana mass (discussed in Eq. (12) of the main text) is

$$M_N < (8\pi^2\rho_\Phi)^{1/4} \simeq 0.12 \text{ eV}, \quad (20)$$

when  $\rho_\Phi$  is set to the present-day dark matter density,  $\rho_{\text{dm}}^0$ . A similar analysis for the quartic coupling applies to the early universe epoch. Moreover, the coupling  $y$  may also be constrained by majoron-emitting decays [47], although these bounds can vary depending on the chosen  $\lambda$  value.

*Implications for neutrino oscillations* — A time-dependent Majorana mass term can affect active neutrino masses and flavor oscillations. The eigenvalues of both active and sterile neutrinos depend on the Dirac mass  $m_D$  and the Majorana mass  $M_N$ . If the Majorana mass is small (as shown in Eq. (20)), the variation in the active neutrino mass remains naturally modest. Consequently, its impact on neutrino flavor oscillations is negligible, removing any direct constraints on the Majorana time ratio  $\tau/T$ . A more comprehensive analysis would require the Casas-Ibarra parameterization [63] of the Yukawa matrix and Dirac mass term in terms of  $M_N$  for all generations, but we do not discuss those details here.

*Implications for cosmology* — Over the cosmic history, the wave DM amplitude  $\Phi_{\text{max}}$  evolved with the universe expansion. Since  $\Phi_{\text{max}} \propto \sqrt{2\rho_\Phi} \sim a^{-3/2}$ , with the scale factor  $a$ , it was much larger at earlier times. As a result,  $-\mu_0^2 \ll g\Phi_{\text{max}}^2$ . Consequently, from Eq. (10) in the main text, the symmetry-broken phase persisted for an extremely short time,  $\tau/T \ll 1$ . This short symmetry-broken interval implies that, for most of the time, the potential remained in the symmetry-restored phase and was dominated by thermal effects, similar to standard early universe phase transitions.

Because neutrinos primarily remained in the Dirac phase at high temperatures, baryogenesis through leptogenesis is disfavored in this scenario. Meanwhile, the singlet scalar mass, effectively  $m_\phi^2 \sim g\Phi_{\text{max}}^2$ , was very large in the early universe, significantly suppressing  $\phi$  production and rendering its contribution to the dark matter relic abundance negligible. Its present-day oscillation amplitude is also negligible, given the extremely low current density.

In the early universe, the large Hubble parameter prevented the singlet scalar  $\phi$  from satisfying the fast-roll condition (16). The scale factor  $a_*$  at which fast-roll of

Type oscillation	Quasi-Dirac $\leftrightarrow$ Majorana	Pure Dirac $\leftrightarrow$ Majorana
Variation	Majorana mass $M_N$	Singlet potential $V(\phi)$
Vanishing $M_N$	$M_N = 0$ at an instant	$M_N = 0$ whenever $v_\phi = 0$
Modulation behavior	LNV (e.g. $0\nu\beta\beta$ decay)	$C\nu B$ or $X \rightarrow Y + \nu\bar{\nu}$

TABLE I. Comparison between quasi-Dirac/Majorana type oscillation [37] and pure Dirac/Majorana type oscillation.

the singlet begins is approximately given by

$$\frac{a_*}{a_{\text{eq}}} \simeq \begin{cases} \left( \frac{H_{\text{eq}}^{7/2} M^{1/2}}{2g\rho_{\text{dm}}^0} \right)^{1/4} & \text{if } H_{\text{eq}}^{3/2} M^{5/2} < 2g\rho_{\text{dm}}^0, \\ \frac{H_{\text{eq}}^2 M^2}{2g\rho_{\text{dm}}^0} & \text{if } H_{\text{eq}}^{3/2} M^{5/2} > 2g\rho_{\text{dm}}^0, \end{cases} \quad (21)$$

where  $a_{\text{eq}}$  and  $H_{\text{eq}}$  denote the scale factor and Hubble parameter at matter-radiation equality, respectively, and  $\rho_{\text{dm}}^0$  is the present-day local dark matter density. In the first case,  $a_*$  precedes the onset of wave DM oscillations, whereas in the second case,  $a_*$  occurs later. In our benchmark parameter setup (see Fig. 3 in the main text), fast-roll begins at  $a_* \sim 10^{-8}$ , while wave DM oscillations start at  $a \sim 10^{-3}$ .

To avoid a large fluctuating vacuum energy, the vacuum energy difference  $\Delta V_0$  between the singlet scalar potential's symmetry-broken and restored phases must remain below the energy density associated with the cosmological constant  $\Lambda$ . Concretely, we impose the condition (purple bound in Fig. 2 of the main text)

$$\Delta V_0 \sim \frac{(-\mu_0^2)^2}{\lambda} < \rho_\Lambda = \frac{\Lambda}{8\pi G} \sim 10^{-47} \text{ GeV}^4, \quad (22)$$

where  $\rho_\Lambda$  is the vacuum energy density. In our benchmark scenario, the vacuum energy difference is  $\Delta V_0 \sim 10^{-53} \text{ GeV}^4$ , which easily satisfies this bound.

*Domain walls* — The breaking of a discrete symmetry can produce domain walls as topological defects [64]. To avoid a cosmological problem, the domain wall energy within the current horizon,  $\sigma_{\text{dw}} H_0^{-2}$ , must be much smaller than the total energy of the present horizon,  $\rho_c H_0^{-3}$ . Here,  $\sigma_{\text{dw}} = \frac{2\sqrt{2}}{3} \lambda^{1/2} v_\phi^3$  is the surface energy density of the domain walls, and  $\rho_c$  is the critical energy density of the universe. This requirement simplifies to  $\sigma_{\text{dw}} \ll \rho_c H_0^{-1} \sim (10 \text{ MeV})^3$ .

A stronger bound arises from domain wall formation in the early universe. To avoid any additional source of CMB anisotropy, we require  $\sigma_{\text{dw}} \lesssim (1 \text{ MeV})^3$  [64, 66, 67].

In our scenario, when the singlet  $\phi$  acquires a nonzero VEV ( $\mu_{\text{eff}}^2 = \mu_0^2 + g\Phi^2 < 0$ ), the surface energy density is bounded above by

$$\sigma_{\text{dw}} = \frac{2\sqrt{2}}{3} \frac{(-\mu_0^2 - g\Phi^2)^{3/2}}{\lambda} < \frac{2\sqrt{2}}{3} \frac{(2\rho_\Phi)^{3/4}}{\lambda^{1/4}}, \quad (23)$$

at all times in cosmic history, as implied by the first inequality in Eq. (12) of the main text. Furthermore, if all conditions for the potential oscillation at present time are satisfied, the maximum possible value of  $\sigma_{\text{dw}}$  remains below the cosmological bound as long as  $\lambda \gtrsim 10^{-88}$ .

Because of this upper bound, domain-wall constraints are weaker than those shown in Fig. 2 of the main text. Adopting the values of  $\mu_0$  and  $\lambda$  from the benchmark scenario in Fig. 3, the surface energy density is estimated to be  $\sigma_{\text{dw}} \sim 10^{-9} \text{ eV}^3$ , which is extremely small.

The dynamics of domain walls under repetition of the symmetry restoration and breaking may differ from the standard scenario. Depending on the oscillation frequency, domain walls may fail to form or might be annihilated, potentially alleviating any cosmological issues. However, we do not analyze these effects in detail here.

Lastly, domain wall fluctuations can evolve alongside density perturbations, remaining compatible with observed large-scale structure [68, 69]. Moreover, gravitational waves may be produced when the domain walls annihilate, providing a possible observational signature for the proposed potential oscillation scenario.

*Comparison between type oscillation scenarios* — Table I contrasts the quasi-Dirac/Majorana oscillation of Ref. [37] with the pure Dirac/Majorana oscillation studied here. In the former, the oscillation stems from a time-varying mass term, whereas in our case it arises from an oscillating potential.

An important distinction lies in the duration for which  $M_N$  vanishes. In quasi-Dirac/Majorana oscillations, the neutrino becomes pure Dirac only at the instant when the value of the oscillating wave DM  $\Phi(t)$  is zero. In contrast, in our scenario, the neutrino remains pure Dirac for a finite interval when the singlet potential is in the symmetry-restored phase and the Majorana mass is zero.

In the quasi-Dirac and Majorana type oscillation scenario, the requirement  $m_\nu < \mathcal{O}(0.1 \text{ eV})$  forces the quasi-Dirac interval to be short on average. However, in our scenario of pure Dirac and Majorana type oscillations, there is no restriction on the Majorana time ratio due to the small scale of  $M_N$  from Eq. (20).

These two scenarios also manifest modulation in different physical processes. Quasi-Dirac/Majorana oscillations modulate lepton-number-violating reactions, whereas oscillations featuring a pure Dirac phase modulate the detection of the cosmic neutrino background, as we discussed in the main text.

Beyond cosmic neutrinos, neutrino-antineutrino pair

emission processes,  $X \rightarrow Y + \nu\bar{\nu}$  [58], can distinguish pure Dirac from Majorana neutrinos in principle because, in the Majorana case, the amplitude is antisymmetric under  $\nu \leftrightarrow \bar{\nu}$  exchange [62]. Examples include  $Z \rightarrow \nu\bar{\nu}$  [59],  $K^+ \rightarrow \pi^+ \nu\bar{\nu}$  [60],  $B^0 \rightarrow \mu^- \mu^+ \nu\bar{\nu}$  [62], and the radiative emission of a neutrino pair [61]. The resulting difference in amplitudes is proportional to  $m_\nu^2$  [62]:

$$\int (|\mathcal{M}_D|^2 - |\mathcal{M}_M|^2) d^4 p_1 d^4 p_2 \propto m_\nu^2, \quad (24)$$

where  $\mathcal{M}_D$  and  $\mathcal{M}_M$  denote the Dirac and Majorana

amplitudes, respectively, and  $p_{1,2}$  are the 4-momenta of the emitted (anti)neutrinos.

In quasi-Dirac/Majorana oscillations, these pair-emission processes exhibit no significant modulation because the neutrino is pure Dirac only at the instant wave DM field value is zero. In contrast, in our pure Dirac/Majorana type oscillation, the neutrino can remain Dirac for a finite interval, allowing for a potential modulation of such processes. Nevertheless, the overall effect remains small, as it is proportional to the square of the active neutrino mass.